Egyptian Journal of Biology, 2009, Vol. 11, pp 13-25
© Printed in Egypt. **Egyptian British Biological Society (EBB Soc)**

Histological and histochemical study on the effect of Ehrlich ascites carcinoma on the liver and kidney of mice and the possible protective role of tetrodotoxin.

Samia M Abd El-Wahab [1] & Fatma M Fouda [2*]
1. Zoology Department, Faculty of Science, Al-Azhar University (Women), Cairo.
2. Zoology Department, Women's College, Ain Shams University, Cairo.

Abstract

Many of the anti cancer drugs in use known to produce undesirable side effects such as hepatotoxicity and renal toxicity. This work was carried out to ascertain the effect of Ehrlich ascites carcinoma on the mice liver and kidney, and to evaluate the possible protective role of tetrodotoxin extracted from the puffer fish (*Arothron diadematus*) from the Red Sea. Experimental mice were divided into six equal groups and injected intra-peritoneally with three levels of toxin (zero; low[$^1/_{20}$ LD_{50}]; high [$^1/_{10}$ LD_{50}]) and two levels of carcinoma cells (zero; two million cells) in a factorial design. Subsets of mice from each group were dissected after 3, 6, 9 and 12 days and liver and kidney sections prepared for histological and histochemical examination. There were hepatic and renal toxic effects induced by carcinoma cells: vacuolated cytoplasm with deeply stained pyknotic nuclei of hepatocytes, large areas of hemorrhage in the kidney, and a highly significant increase in glycogen content. These negative effects were relieved for 3 or 6 days after injection by the low dose of toxin. This raises the possibility of including tetrodotoxin in a successful therapeutic regimen against cancer.

Keywords: Cancer, sodium channel blockers, liver, kidney, histopathology.

Introduction

Cancer is one of the major causes of death. For cancer, the general conventional treatment and standard of care for clinical oncology remains surgery followed by radiation and / or systemic chemotherapy as deemed appropriate based on the clinical findings (Samanta *et al*. 2007).

Most anti-cancer agents eradicate tumor cells by the induction of apoptosis. Recent studies have suggested that the various anti-cancer agents used against cancer mediate their effects by induction of apoptosis of the cancer cells (Ferreria *et al*. 2002; Debatin *et al*. 2002; Bhattacharyya *et al*. 2003; Norbury & Zhivotovsky 2004; Fouda 2005). The basic aim in the use of anti-cancer agents is to inhibit the proliferation of tumor cells or kill them without damaging the normal cells. Among the most effective methods of treatment is the use of natural products which prove in many cases to have many fewer side-effects than chemical or radioactive treatments. A large number of natural products have been studied for anti-cancer activity on various experimental models. This has resulted in the availability of nearly 30 effective anti-cancer drugs (Ramakrishna *et al*. 1984; Ramnath *et al*. 2002; Bhattacharyya *et al*. 2007; Chakraborty *et al*. 2007; Lee *et al*. 2007).

Tetrodotoxin (anhydrotetrodotoxin 4-epitetrodotoxin, or tetrodonic acid) is among the deadliest toxins known to man. It can be isolated from many tissues (liver, intestine, gonads, kidney and skin) of the puffer fish or fugu (*Arothron diadematus*: Tetraodontidae). It is a reversible selective inhibitor of sodium channel conductance (Kao 1966, 1972). Only one study has been performed in animals to test the antinociceptive properties of tetrodotoxin in neuropathic and cancer pain (Lyu *et al*. 2000). Tetrodotoxin diminished pain behaviour in a dose-dependent manner in models of inflammatory, visceral and neuropathic pain without causing adverse events (Marcil *et al*. 2006). Unlike other analgesics, such as morphine, tetrodotoxin affects the body in a highly targeted way, by blocking certain subtypes of sodium channels in cell membranes. It seems that tetrodotoxin blocks those sodium channels needed to transmit pain signals in the body (Hagen *et al*. 2005).

Fouda (2005) demonstrated the apoptogenic effect of tetrodotoxin to tumour-bearing mice. She showed that the anti-tumor activity of tetrodotoxin increased lifespan in addition to

* Address for correspondence. Email *momouk@hotmail.com*

decreasing the number of tumor cells. There was also an obvious effect of tetrodotoxin on cells, leading to apoptosis and a decrease in the volume of the peritoneal fluid. The present study was carried out to investigate this possible protective role of tetrodotoxin in tumour-bearing mice.

Materials & Methods

Adult female Swiss albino mice (20-25g) were obtained from the animal house of the National Cancer Research Institute (Kasr El-Ainy St, Cairo, Egypt). About 130 mice were used in this study. They were housed in stainless steel boxes in a controlled environment (temperature 20±2 ◦C and 12D:12L daylength) with standard laboratory diet and water *ad libitum* at the animal facility of the Women's College, Ain Shams University.

We used Ehrlich ascites carcinoma (EAC) as a model for testing the effects of tetrodotoxin: this model has been shown by many authors to give accurate and reliable results in anti-cancer research (Sheeja *et al*. 1997; Ramnath *et al*. 2002; Gupta *et al*. 2004; Fouda 2005). Its reliability lies in its ability to determine the value of any anti-cancer drug through estimates of the prolongation of experimental lifespan, changes in the number and viability of the cell line itself, and the volume of the liquid generated by the tumor inside the peritoneal cavity (Maity *et al*. 1999). EAC cells (ECACC 87032503) were obtained from the National Cancer Research Institute, via a 25 g female albino mouse. They were maintained by weekly interaperitoneal inoculation of saline solution containing 10^6 cells /mouse.

The skins of five masked puffer fish (*Arothron diadematus*) were prepared using acidified methanol extract solution according to the method of Kawabata (1978). The extract was then boiled for 10 min, cooled, centrifuged at 1000 rpm for 3-5 min and the supernatant containing the tetrodotoxin stored at -4◦C until used. The toxicity of the tetrodotoxin extracted from the fish skin was determined (in mouse units) according to the method described by Kawabata (1978). A series of concentrations were injected interaperitoneally into 20 g male albino mice obtained from the animal house of Theodor Belharis Institute. One mouse unit is defined as the amount of toxin required to kill a 20 g mouse within 30 min. The LD_{50} of the extracted tetrodotoxin was also determined according to the method of Behreus & Karbeur (1953) (determined after 96 h).

Animals were divided into six equal groups, 20 mice each. All mice received the carrier (injection of 0.9% sodium chloride solution) on the first day of the experiment; treatments involved two factors in a two-way factorial design: *toxin* (with three levels: 1 -zero, 2 - low [an injection of $^1/_{20}$ LD_{50} on the first day of the experiment] and 3 - high [an injection of $^1/_{10}$ LD_{50} on the first day of the experiment]) and *EAC* (with two levels: A - zero, and B - inoculation with 1×10^6 EAC cells on the first day of experiment). Groups are referred to by the group combination (eg group 1A is the control group, with no toxin and no EAC cells injected).

Five animals from each group were dissected on each of the days 3, 6, 9 and 12 after the inoculation and injection. Livers and kidneys were surgically excised, then fixed in neutral formalin. Sections 5 µ thick were then cut and stained with H & E (Drury & Wallington 1980), Masson's trichrome (Kiernan 1999) and PAS-stain (Drury & Wallington 1980).

The photographs of PAS-stained sections were analyzed using Image–Pro-Plus software. Ten fields were randomly chosen in each group. The data were analysed as a three-way Analysis of Variance (day x EAC x TTX) using Minitab 13.

Results

The results of toxicity experiment showed that 3 mg of extract was sufficient to cause death of a 20-g mouse in 30 min (one mouse unit). The results of the 96-h LD_{50} experiment showed that

0.35 ± 0.02 mg was sufficient to kill 50% of the animals. Accordingly, the doses used in the experiments were 0.0350 and 0.0175 mg, representing $^{1}/_{10}$ and $^{1}/_{20}$ LD_{50}. In normal tetrodotoxin-treated subjects, all injected animals exhibited some symptoms of toxicity, such as slow movement, hair erection and loss of appetite.

The liver of control mice (group 1A) appeared to be formed of the classical hepatic lobules. Each lobule showed radially arranged hepatocytes forming cords around the central veins. Hepatocytes appeared polygonal in shape with rounded central vesicular nuclei. Blood sinusoids were seen separating the cords of the liver cells and lined by flattened endothelial cells and Von Kupffer cells (Fig. 1). Minimal amount of thin fine collagen fibers was seen around the central veins and portal areas (Fig. 2). Hepatocytes showed an intense PAS positive reaction (Fig. 3).

Examination of sections of group 2A and group 3A, which received an injection of $^{1}/_{20}$ and $^{1}/_{10}$ LD_{50} of tetrodotoxin respectively, showed no histological differences in comparison with the control group (Fig. 4).

Most of the hepatocytes of Group 1B sections had vacuolated cytoplasm and deeply stained nuclei after 6 days of inoculation (Fig. 5). Masson's trichrome-stained sections showed apparent increases in collagen content around the central veins 6 days after inoculation (Fig. 6). PAS-stained sections showed intense PAS-positive reactions in the hepatocytes 3 days after inoculation (Fig. 7), confirmed by optical density measurements (Table 1).

Table 1: Mean optical density values of PAS-positive material in mice liver. Each value is a mean ± SE (n = 10)
The 3-way ANOVA showed a very highly significant three-way interaction of *day x EAC x TTX* ($F_{6,216}$ = 20.4, p<0.001), indicating that the time course was strongly affected by the presence of EAC and of TTX, and that the factors of EAC and TTX interacted non-linearly.

	Days post-inoculation	1: Control	2: $^{1}/_{20}$ LD_{50} TTX	3: $^{1}/_{10}$ LD_{50} TTX
A: no EAC	3	274.1 ± 2.80	289.0 ± 1.83	290.1 ± 1.79
	6	285.9 ± 1.93	277.3 ± 1.99	281.0 ± 2.05
	9	283.4 ± 3.66	297.6 ± 3.45	292.3 ± 3.22
	12	281.3 ± 2.04	292.6 ± 1.89	285.0 ± 1.90
B: EAC	3	359.3 ± 2.85	350.5 ± 2.98	341.1 ± 2.77
	6	372.0 ± 1.21	292.5 ± 3.08	289.2 ± 1.85
	9	390.0 ± 1.47	379.6 ± 4.04	384.1 ± 1.88
	12	363.0 ± 2.51	361.4 ± 3.25	355.6 ± 2.80

In group 2B, nine days after treatment, sections showed vacuolated and necrosis in the cytoplasm with deeply stained pyknotic nuclei (Fig. 9). A widening of the portal tract and mononuclear cellular infiltration around the congested portal vein were seen after 12 days of treatment (Fig. 10). The cellular architecture of the hepatic lobules seemed to have only a few altered hepatic cell foci 6 days after treatment (Fig. 8). The cells were positively stained with H & E and the cytoplasmic material was less vacuolated. Minimal collagen fibers were seen around the central vein, similar to the control (1A) group (Fig. 11). PAS-stained sections showed an intensified heterogeneous staining reaction within lobules (Fig. 12) 6 days after treatment, nearly the same distribution of PAS positive material as in the control group. Optical density measurements showed highly significant increases in PAS-positive material post inoculation (Table 1). However $^{1}/_{20}$ LD_{50} TTX resulted in non significant difference in the density 6 day after treatment compared to the control (1A) group.

In Group 3B, 6 days after treatment liver sections revealed that the hepatocytes had vacuolated cytoplasm and pyknotic nuclei (Fig. 13) and the portal vein was congested. Optical

density measurements showed highly significant increases in PAS-positive material post inoculation (Table 1). However $^{1}/_{10}$ LD_{50} TTX resulted in non-significant difference in the density 6 day after treatment compared to the control group (1A).

In the kidney, the renal cortex of control mice (1A) showed that the renal corpuscles were formed of lobulated glomeruli surrounded by Bowman's spaces. The proximal convoluted tubules appeared to be lined by a single layer of cuboidal epithelium enclosing a narrow lumen. The distal convoluted tubules were lined by cubical cells surrounding wider lumina (Fig. 14). Masson's trichrome-stained sections showed scanty collagen content in the glomeruli and in the interstitial tissue (Fig. 15). Both proximal and distal tubules showed distinct PAS-positive basement membranes, and the proximal tubules also had a PAS-positive brush border (Fig. 16).

Table 2: Mean optical density values of PAS-positive content in mice kidney. Each value is a mean ± SE (n = 10)
The 3-way ANOVA showed that there was a very highly significant 3-way interaction of *day x EAC x TTX* ($F_{6,216}$ = 88.5, p<<0.001), indicating that the time course was strongly affected by the presence of EAC and of TTX, and that the factors of EAC and TTX interacted non-linearly.

	Days post-inoculation	1: Control	2: $^{1}/_{20}$ LD_{50} TTX	3: $^{1}/_{10}$ LD_{50} TTX
A: no EAC	3	203.0 ± 1.92	200.3 ± 1.02	209.0 ± 1.52
	6	211.3 ± 1.75	206.9 ± 1.18	209.1 ± 1.69
	9	220.1 ± 1.14	215.7 ± 1.63	234.3 ± 2.99
	12	223.9 ± 1.16	220.7 ± 1.04	204.6 ± 1.74
B: EAC	3	252.5 ± 3.07	220.1 ± 1.86	220.9 ± 1.77
	6	256.3 ± 1.60	264.7 ± 2.34	260.8 ± 1.20
	9	263.2 ± 1.21	271.1 ± 1.97	211.3 ± 1.06
	12	255.9 ± 1.18	266.7 ± 1.05	252.0 ± 1.17

Groups 2A and 3A showed no histological changes in comparison to the control group (1A) (Fig. 17). Group 1B sections revealed congestion of blood vessels (Fig. 18) 3 days after inoculation. Large areas of interstitial haemorrhage were also seen after 9 days (Fig. 19). Masson's trichrome-stained sections showed many collagen fibers surrounding some renal corpuscles and in the interstitium between some densely stained renal tubules (Fig. 20). Mild increases in PAS-positive reactions were observed at the brush borders of the proximal tubules 3 days after inoculation (Fig. 21). Optical density measurements showed that EAC inoculation generally caused highly significant increases in PAS-positive material in all sampled times relative to the control (Table 2).

In group 2B, 9 days after treatment the histological picture was nearly the same as the control (1A) group (Fig. 22). Masson's stained sections appeared very similar to the control group (Fig. 23). PAS-stained sections showed nearly the same distribution of PAS-positive material (Fig. 24). The optical density values showed a highly significant increase post inoculation (Table 2).

Group 3B sections had areas of haemorrhage, swelling of the epithelial cells of the proximal tubules with disappearance of their lumina (Fig. 25) 12 days after treatment. Interstitial lymphocytic infiltration was also noticed. The optical density values showed a highly significant increase post-inoculation (Table 2). However, $^{1}/_{10}$ LD_{50} TTX resulted in non-significant difference in the density of PAS-positive material 9 days after treatment when it was compared to control (1A) group.

Fig. 1: Liver section of a control mouse showing branching and anastomosing cords of hepatocytes radiating from the central vein (CV).The hepatocytes have vesicular nuclei and some are binucleated. Cells are separated by sinusoids (S) lined by flat endothelial cells and Von Kupffer cells (arrows). (Group 1A, H&E, x200)

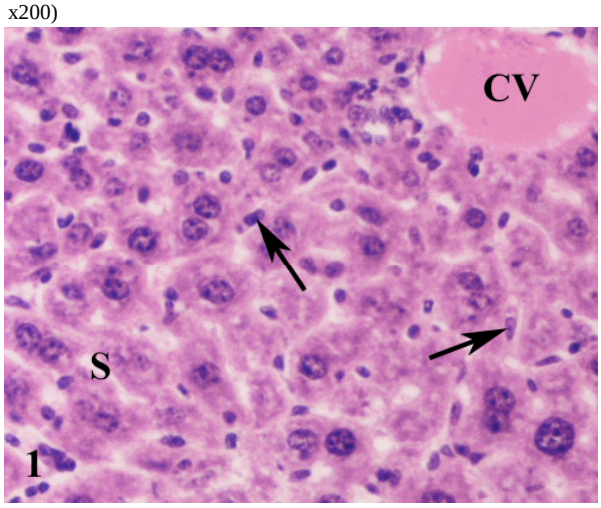

Fig. 2: Liver section of a control mouse showing few collagen fibers around the central vein (arrow) and the outer surface of the blood sinusoids (S). (Group 1A, Masson's trichrome, x400)

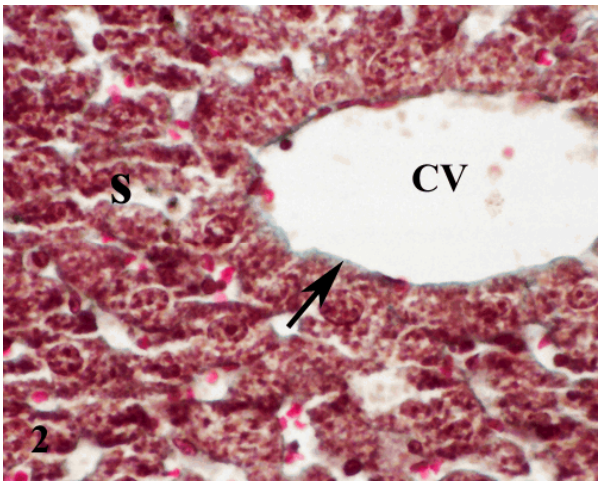

Fig. 3: Liver section of a control mouse showing normal glycogen content. The glycogen granules are seen accumulating at the sides of the hepatocytes. (Group 1A, PAS, x200)

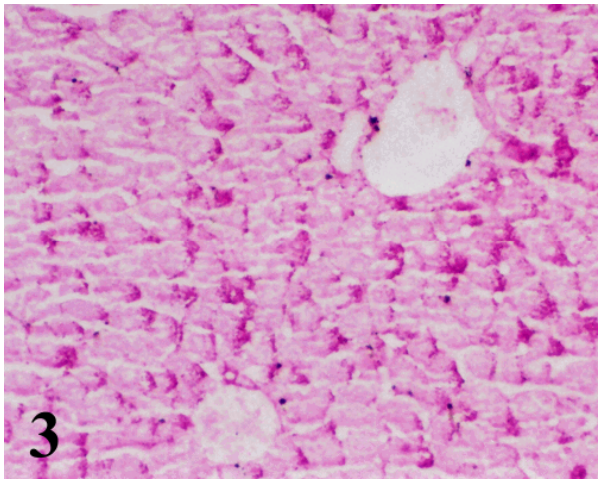

Fig. 4: Liver section of mouse after six days of injection of $^{1}/_{10}$ LD_{50} of tetrodotoxin showing no prominent histological changes. (Group 3A, H&E, x200)

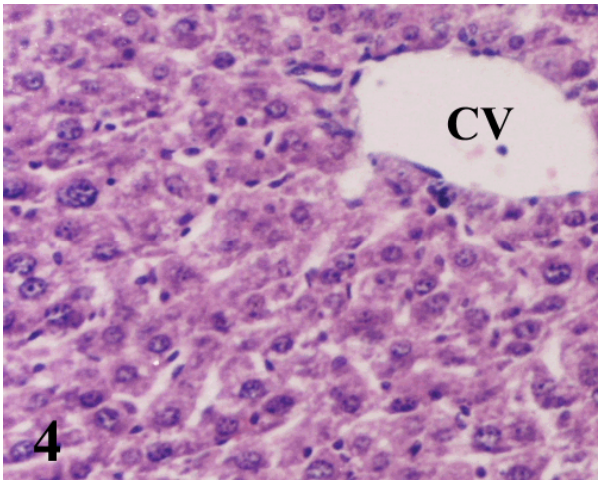

Fig.5: Liver section of mouse after six days of EAC cells inoculation displaying hypertrophy of liver cells, necrosis (N) and most of the hepatocytes have vacuolated cytoplasm with deeply stained pyknotic nuclei (arrows). (Group 1B, H&E, x200)

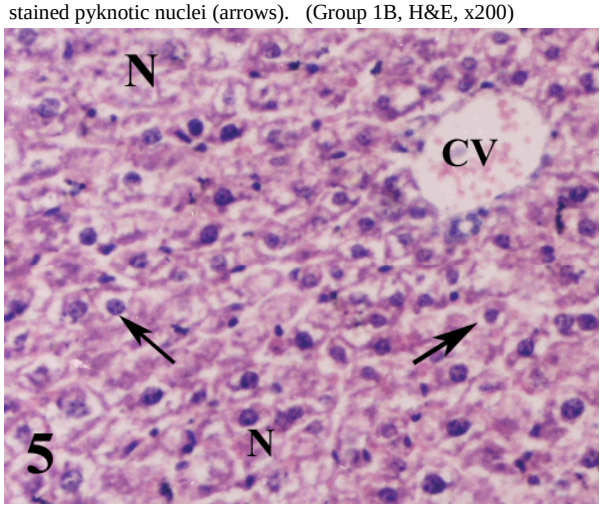

Fig. 6: Liver section of mouse after 6 days of EAC cells inoculation showing an increase in the collagenous fibers around the congested central vein (arrow) and blood sinusoids (S). (Group 1B, Masson's trichrome, x400)

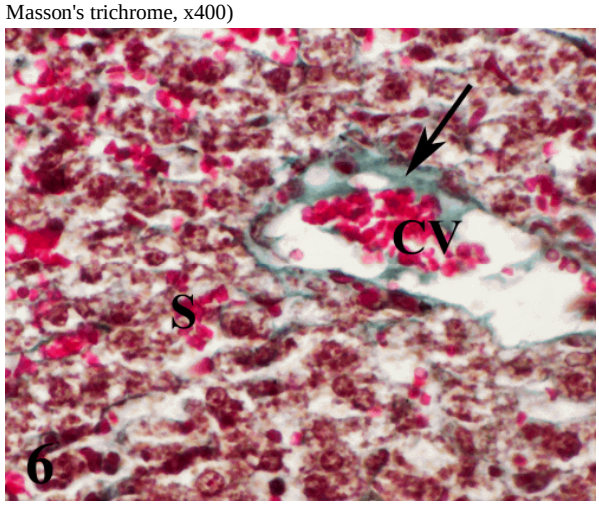

Fig.7: Liver section of mouse after three days of EAC cells inoculation demonstrating marked increase of glycogen in the hepatocytes. (Group 1B, PAS, x200)

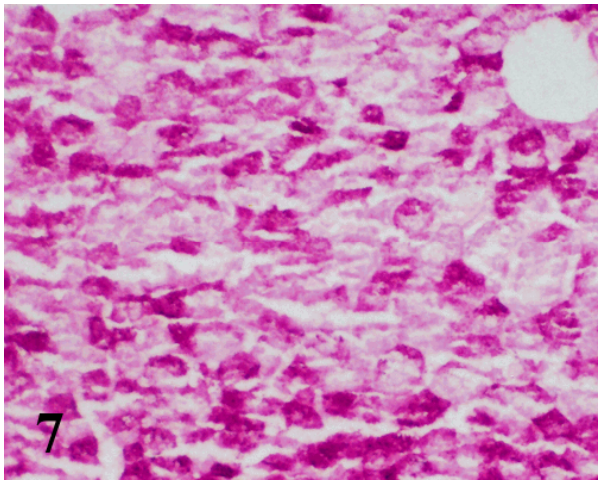

Fig.8: Liver section of mouse after six days of EAC cells inoculation and injection of $^{1}/_{20}$ LD_{50} of tetrodotoxin showing that the cellular architecture of hepatic lobules presented normal with weakly congested central vein. (Group 2B, H&E, x200)

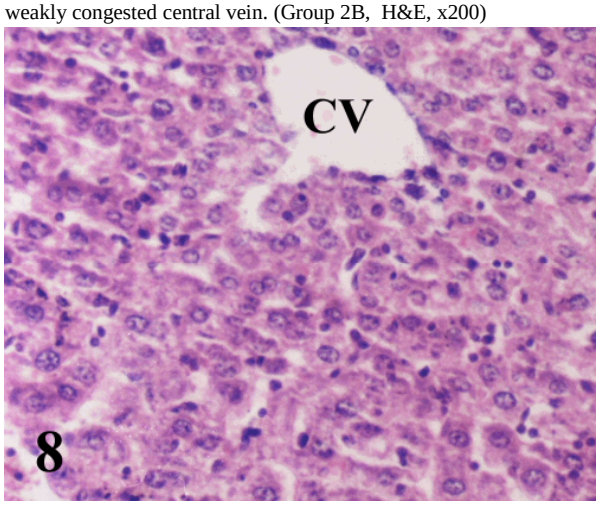

Fig. 9: Liver section of mouse after nine days of EAC cells inoculation and injection of $^{1}/_{20}$ LD_{50} of tetrodotoxin showing focal areas of necrosis (N),congested central vein (CV) and most of hepatocytes with vacuolated cytoplasm and deeply stained pyknotic nuclei (arrows). (Group 2B, H&E, x200)

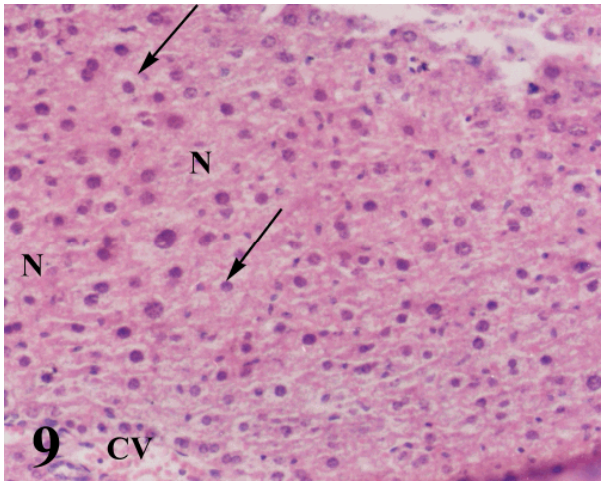

Fig. 10: Liver section of mouse after the 12th days of EAC cells inoculation and injection of $^{1}/_{20}LD_{50}$ of tetrodotoxin showing vacuolated hepatocyte nucleus (arrow head), widen portal tract with dilated congested portal vein (PV) and mononuclear cellular infiltration (arrow). (Group 2B, H&E, x200)

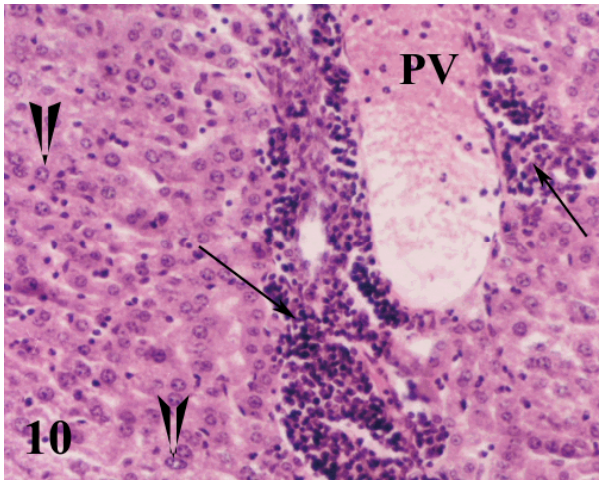

Fig. 11: Liver section of mouse after six days of EAC cells inoculation and injection of $^{1}/_{20}$ LD_{50} of tetrodotoxin showing scanty amount of collagen fibers around the central vein (arrow) and blood sinusoids (S). (Group 2B, Masson's trichrome, x400)

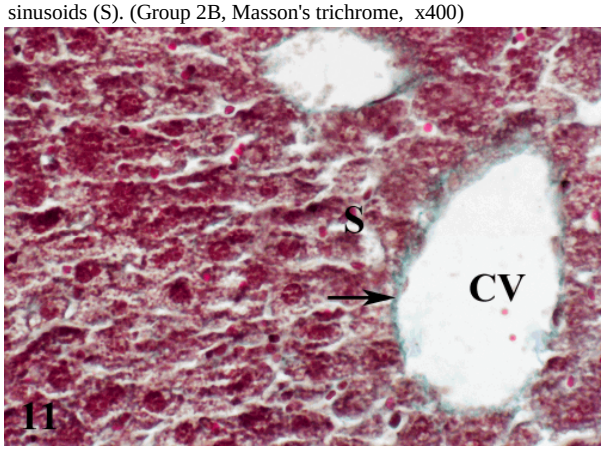

Fig. 12: Liver section of mouse after six days of EAC cells inoculation and injection of $^{1}/_{20}$ LD_{50} of tetrodotoxin showing nearly the same distribution of PAS positive material as in control group. (Group 2B, PAS, x200)

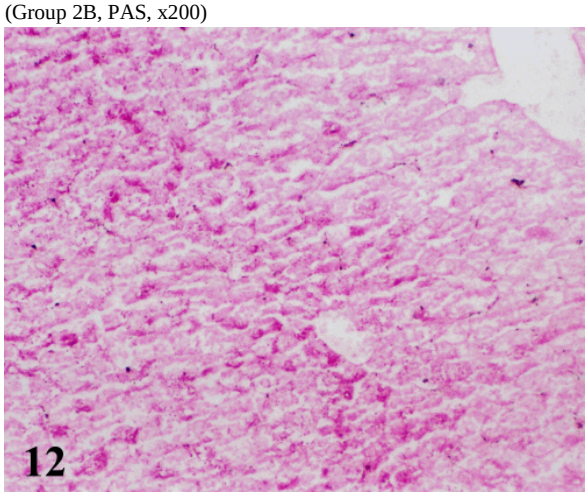

Fig. 13: Liver section of mouse after six days of EAC cells inoculation and injection of $^{1}/_{10}$ LD_{50} of tetrodotoxin showing hepatocytes with vacuolated cytoplasm and karyorrhetic nuclei (arrows) and focal areas of necrosis (N). Notice the congested portal vein (PV). (Group 3B, H&E, x200

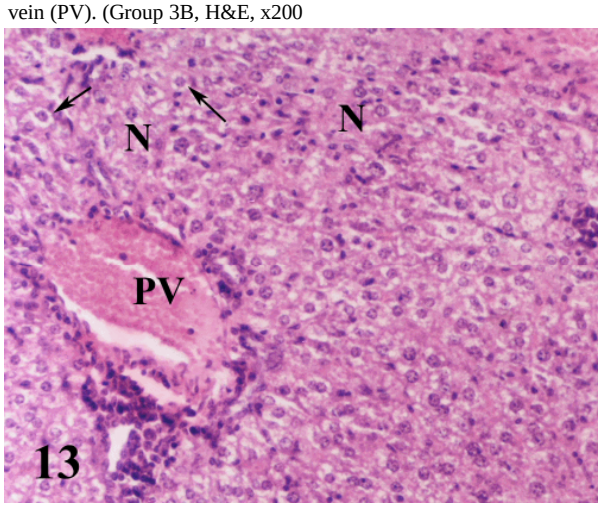

Fig. 14: Section in the renal cortex of a control mouse showing renal corpuscle (C), proximal (P) and distal convoluted tubules (D). (Group 1A, H&E, x 200)

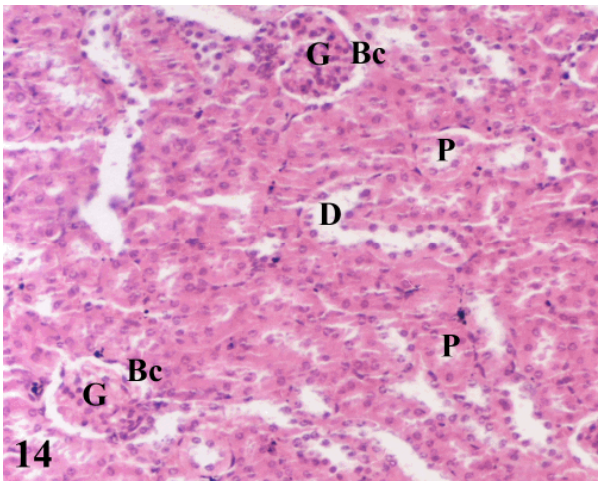

Fig. 15: Section in the renal cortex of a control mouse showing scanty collagen content in the glomeruli and in the renal interstitium. (Group 1A, Masson's trichrome, x400)

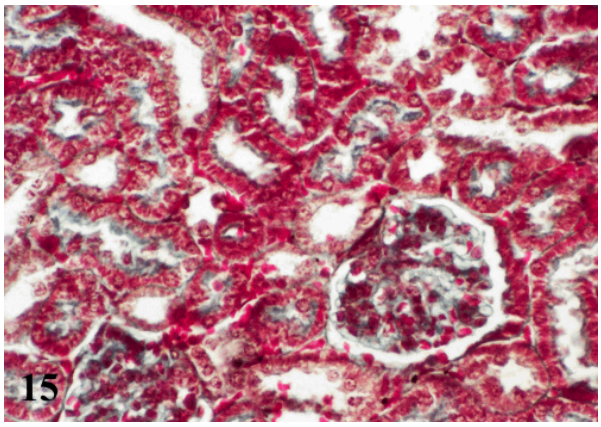

Fig. 16: Section in the renal cortex of a control mouse showing PAS positive material in the basement membranes of the renal structures as well as in the brush borders of the proximal convoluted tubules epithelium. (Group 1A, PAS, x200)

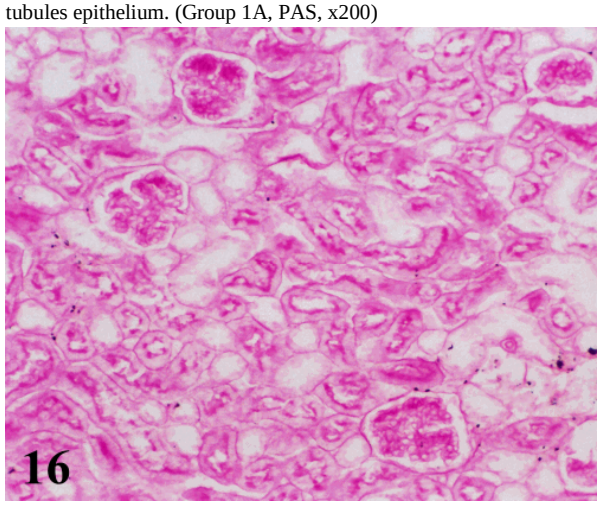

Fig.17: Section in the renal cortex of mouse after nine days of injection of $^{1}/_{10}$ LD_{50} of tetrodotoxin showing nearly the same histological profile as in control group. (Group 3A, H&E, x200)

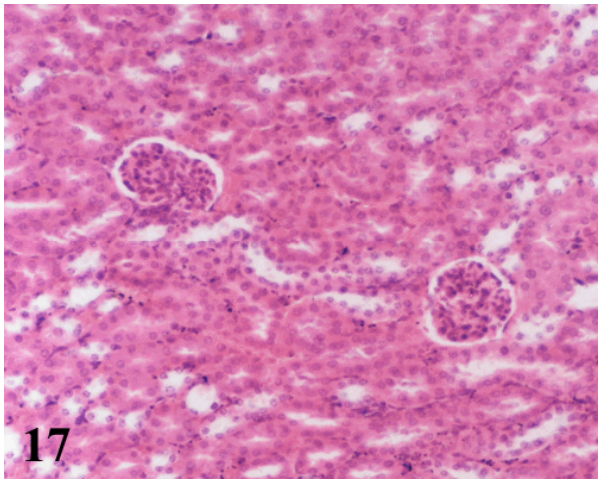

Fig. 18: Section in the renal cortex of mouse after three days of EAC cells inoculation displaying glomerular debris with ruptured Bowman's capsule (Bc) and congestion of blood vessels (arrow). (Group 1B, H&E, x200)

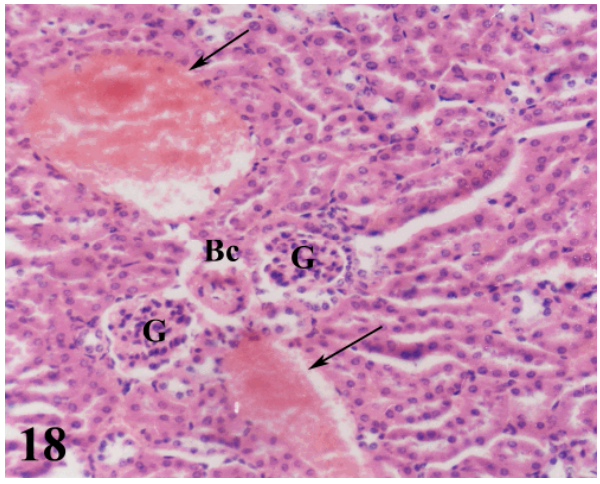

Fig. 19: Section in the renal cortex of mouse after nine days of EAC cells inoculation showing a large area of interstitial hemorrhage (h) and glomerular atrophy (G). (Group 1B, H&E, x200)

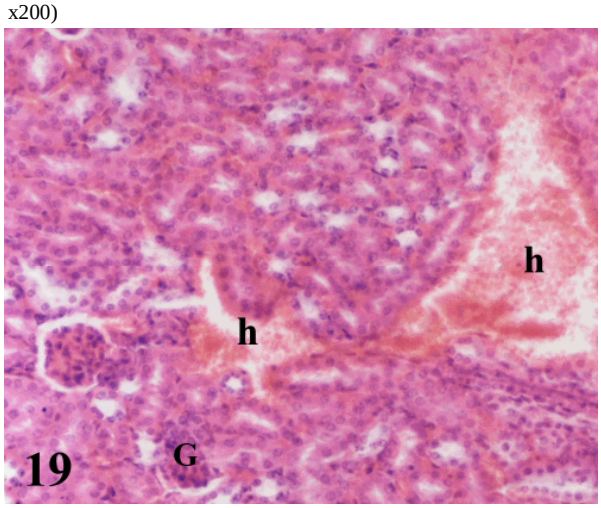

Fig. 20: Section in the renal cortex of mouse after three days of EAC cells inoculation showing congested peritubular blood capillary (arrow) and interstitial fibrosis (double arrow) and hemorrhage (arrow head). (Group 1B, Masson's trichrome x400)

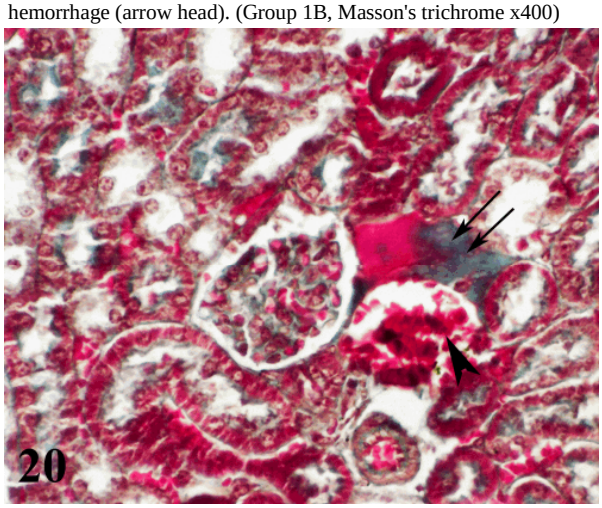

Fig. 21: Section in the renal cortex of mouse after three days of EAC cells inoculation showing intense PAS positive reaction. (Group 1B, PAS, x200)

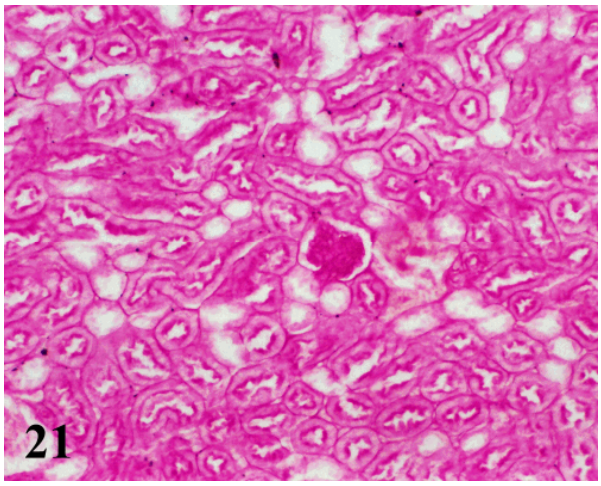

Fig. 22: Section in the renal cortex of mouse after nine days of EAC inoculation and injection of $^{1}/_{20}$ LD_{50} of tetrodotoxin revealing nearly the same histological profile as in control group apart of mild interstitial congestion (arrow). (Group 2B, H&E, x200)

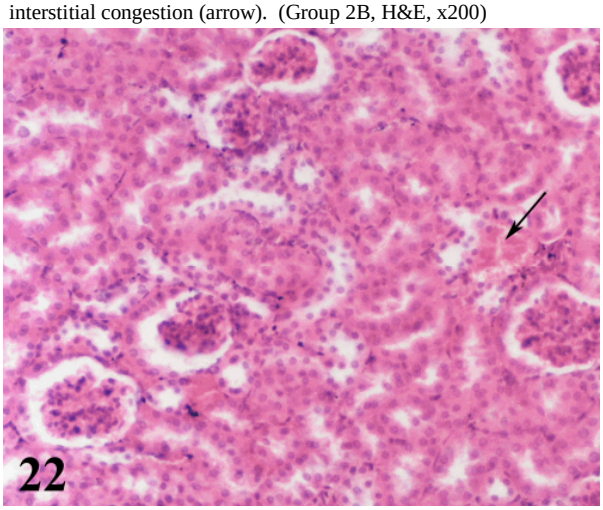

Fig. 23: Section in the renal cortex of mouse after three days of EAC inoculation and injection of $^{1}/_{20}$ LD_{50} of tetrodotoxin which is as normal as control. (Group 2B, Masson's trichrome, x400)

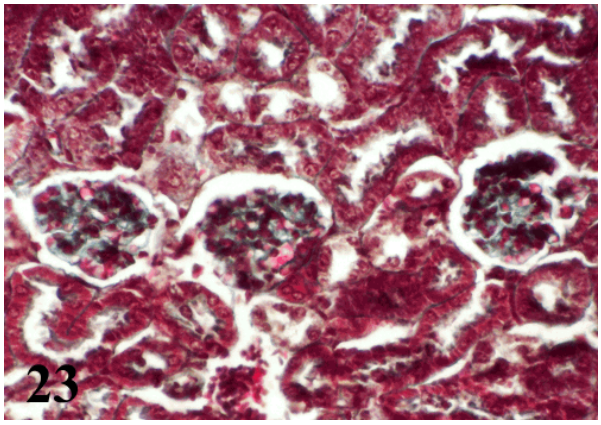

Fig. 24: Section in the renal cortex of mouse after three days of EAC inoculation and injection of $^{1}/_{20}$ LD_{50} of tetrodotoxin showing nearly the same intense reaction of PAS positive material as in control group. (Group 2B, PAS, x200)

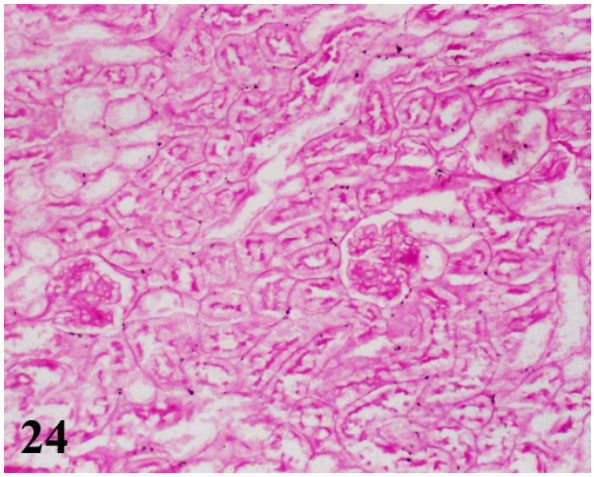

Fig. 25: Section in the renal cortex of mouse after twelve days of EAC inoculation and injection of $^{1}/_{10}$ LD_{50} of tetrodotoxin showing glomerular atrophy and destruction together with interstitial lymphocytic infiltration (arrow) and areas of hemorrhage (h). Notice swelling of the epithelial cells of proximal convoluted tubules (P) with disappearance of their lumina. (Group 3B, H&E, x200)

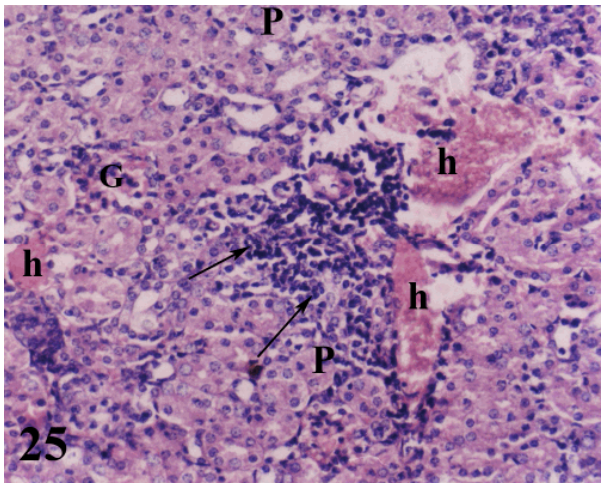

Discussion

In normal tetrodotoxin-treated subjects, all injected animals exhibited some symptoms of toxicity such as slow movement, hair erection and loss of appetite. Preliminary results showed that adverse events consisted of transient perioral numbness or tingling, nausea and ataxia after intra-muscular injection of tetrodotoxin in group of patients suffering from severe cancer pain (Hagen *et al*. 2005). In contrast, the mice injected with tetrodotoxin show free movement throughout (Marcil *et al*. 2006).

The present study showed that the injection of tetrodotoxin alone did not produce any detectable structural changes in the liver and renal tissues. There was accumulation of glycogen. No inflammatory cells could be detected and no collagen fiber deposition. These findings contrast with those of Yamaguchi (1996), where liver and kidney sections showed congestion in mice after intra-peritoneal injection of tetrodotoxin prepared from the ovary of *Takifugu porphyreus*. Cytopathological changes in mice were detected mainly in nerve tissues when a small amount of tetrodotoxin was administered (Yamaguchi 1996).

In the liver sections of the EAC-inoculated animals, hepatocytes showed vacuolar degeneration (hydropic changes) with deeply stained pyknotic nuclei and necrosis. These pathological changes became severe with time, as reported by others (Bhattacharyya *et al*. 2007; Chakraborty *et al*. 2007). This may be due to the accumulation of haemorrhagic ascitic fluid within the peritoneal cavity in which the cells proliferate and move to invade the internal organs (Chakraborty *et al*. 2007).

Acording to Telbisz *et al*. (2001), activation of autophagy is frequently observed in different types of pathological tissue degeneration. It increases in some cases, and lysosomes are responsible for regulated degradation of the autophagic vacuoles. In apoptosis, lysosomes degrade the contents of phagocytic vacuoles derived from engulfed apoptotic blebs. Lysosomal enzymes discharged from disintegrated cells have a key role in the induction of necrotic changes.

EAC-inoculated animals in this study showed increased collagen deposition in the connective tissue surrounding the central veins of the liver and in scattered areas of the interstitium of the renal cortex. Horn *et al*. (1985) declared that the presence of collagen in the perisinusoidal space might affect the blood supply to liver cells and would reduce the exchange

of metabolites, perhaps causing hepatocellular dysfunction and necrosis. Enzan *et al*. (1995) attributed a similar finding to the activation of myofibroblast-like cells present normally within the hepatic and renal parenchyma. George *et al*. (2001) suggested that decreased synthesis of collagenolytic enzymes by the impaired hepatocytes might contribute to further accumulation of collagen. The presence of fibrosis suggests more advanced and severe liver injury (Angulo 2002).

Here, EAC treatment induced a marked increase in the glycogen content of liver cells, previously proposed to be influenced by a depletion of hepatic reduced glutathione (GSH) (Sato & Izumi 1989). Preliminary studies demonstrated that EAC inoculation induced a decrease in hepatic glutathione (GSH) content associated with inhibition of hepatic glutathione peroxidase (GSH_{px}) and superoxide dismutase (SOD) activity (Navarro *et al*. 1999; Farag & Abdel Dayem 2001; Fouda, 2005; Bhattacharyya *et al*. 2007). This reduction in SOD and GSH activity could alter antioxidant defences, resulting in enhanced oxidation due to accumulation of reactive oxygen species and reduction of antioxidants in liver tissues. SOD acts to trap superoxide radicals, while GSH can chemically detoxify H_2O_2. These enzymes serve as a defence system to safeguard cells from the toxic effect of reactive oxygen intermediates (Fouda 2005).

Liver sections of EAC+tetrodotoxin-treated mice revealed the loss of normal appearance, and most hepatocytes showed vacuolated cytoplasm with pyknotic nuclei and necrosis six to nine days after treatment. Lobular infiltration by mononuclear inflammatory cells appeared mainly around the central vein, extending in some specimens to involve the portal area after 12 days. These changes may be due to disorganization of the cytoplasm (Hashimoto *et al*. 1995), or more probably because of mitochondrial degeneration. Necrosis usually involves groups of contiguous cells and leads to hydropic degeneration of the cytoplasm and irreversible failure of cell organelles, both processes believed to be caused by lysosomal enzymes and hydration (Fukuda *et al*. 1993).

In contrast, six days after treatment with EAC + tetrodotoxin, the cellular architecture of hepatic lobules seemed to have few altered hepatic cells. The cells were generally less vacuolated. No inflammatory cells could be detected, and collagen fibers were seen around the central vein, similar to the control group. PAS-stained sections showed nearly the same distribution of glycogen material as in the control group.

Treatment with an anti-tumor dose of tetrodotoxin could replenish the host's antioxidant system, thereby protecting the host's liver and kidney from lipid peroxidation and subsequent degeneration. Thus, unlike many other anti-cancer agents, tetrodotoxin not only has anti-tumor properties, but also protects the host liver and kidney from tumor–induced toxicity.

Adminstration of tetrodotoxin further decreased the viable tumor cell count in EAC-bearing animals (Fouda 2005). This may point toward the underlying chemopreventive potential of tetrodotoxin *in vivo*. Although mechanistic insights into the chemoprevention of tetrodotoxin are unexplored, we may assume that tetrodotoxin–mediated tumor cell apoptosis could be one possible pathway for the decreased number of viable tumor cells.

Reports indicate that many antioxidants are anti-carcinogens (Maxwell 1995). Tetrodotoxin possesses antioxidant properties and may therefore be effective in combating oxidative stress following tumor transplantation. Tetrodotoxin-mediated suppression of tumor peritoneal cell counts and the volume of fluid indicates its anti-tumor activity and chemoprotection therapy. The anti-tumor effect of tetrodotoxin against EAC in mice is reflected in an increase in its mean lifespan by about 28-42%, depending on the dose (Fouda 2005).

Fouda (2005) demonstrated that the administration of tetrodotoxin at $^1/_{10}$ LD_{50} dose to tumor-bearing mice caused a partial improvement in the level of SOD and GSH_{px} in a time-dependent manner, which may highlight the antioxidant and free radical scavenging properties of tetrodotoxin. The mechanism of the potential protective role of tetrodotoxin in ameliorating

the toxic effects of EAC cells is presumably because of its antioxidant and free-radical scavenging properties.

Kidney sections of EAC-inoculated animals showed congestion of blood vessels, glomerular atrophy and dilated proximal tubules three days after inoculation. Large areas of interstitial haemorrhage were also seen after nine days. These pathological changes were severe with time in the EAC–bearing mice. An explanation of the congestion and areas of interstitial haemorrhage may lie in the weakness of the renal parenchymal tissue as a result of the degenerative changes (Holdaas *et al*. 1985). These structural changes reflect upon one or more of the principal functions of the kidneys, which include volume regulation, acid base balance, electrolyte balance, excretion of waste products and endocrine functions including the elaboration of rennin and erythropoietin (Cotran, 1987). The present study showed that EAC cells induced an increase in glycogen content in renal tissue, especially at the brush border of the proximal tubules.

Nine days after treatment with a single intraperitoneal injection of a low dose of tetrodotoxin together with EAC cells, many glomeruli were near to normal size and appearance, but a few were still affected. Renal tubules still showed vacuolar degeneration in some lining epithelial cells. Three days after the same treatment, PAS-stained sections showed nearly the same distribution of glycogen material. The protective effects of tetrodotoxin recorded in this study were in accord with those reported by Fouda (2005), who showed that the injection of tetrodotoxin could reduce tumor peritoneal cell count and fluid volume. As a consequence the proliferation and invasiveness of such cells are suppressed (Grolleau *et al*. 2001). Tetrodotoxin has also shown to be an apoptogenic agent to EAC cells (Fouda 2005). Again, the mechanism of the potential protective role of tetrodotoxin in ameliorating the toxic effects of EAC cells is presumably due to its antioxidant properties (Fouda 2005).

High doses of tetrodotoxin together with EAC cells produced areas of haemorrhage, swelling of some renal proximal-tubule cells and interstitial lymphocytic infiltration 12 days after treatment. It is possible to say that the interstitial lymphocytic infiltration is an indication of an inflammatory process, while the swelling of the epithelial cells of the proximal tubules could be an indication of regenerative changes in these tubules.

Thus treatment with low doses of tetrodotoxin remarkably ameliorates some of the histopathological features manifested in rat kidneys inoculated with EAC cells. Such effects were noted in both Malpighian corpuscles and kidney tubules. In conclusion, tetrodotoxin appears to be useful in reducing both hepatic and renal oxidative damage.

Acknowledgments

We thank Dr. Mohamed Abou Zaid, Professor of Aquatic Biology, Zoology Department, Faculty of Science, Al-Azhar-University (Men's section) for his valuable comments on the manuscript. Sincere thanks to Dr. Mona El-Tonsy, Professor of Histology and Cytology and Head of Zoology Department, Faculty of Science, Al-Azhar University (Women's section) for her advice and for reading the paper.

References

Angulo P (2002) Nonalcoholic fatty liver disease. *New England Journal of Medicine* 346(16): 1221-12231.

Behreus AS & Karbeur L (1953) Determination of LD_{50}. *Archiv für experimentelle Pathologie und Pharmacie* 28: 177-183.

Bhattacharyya A, Choudhuri T, Pal S, Chattopadhyay S, Datta GK, Sa K & Das T (2003) Apoptogenic effects of black tea on Ehrlich's ascites carcinoma cells. *Carcinogenesis* 24 (1): 75-80.

Bhattacharyya A, Mandal D, Lahiry L, Bhattacharyya S, Chattopadhyay S, Ghosh UK, Sa G & Das T(2007) Black tea-induced amelioration of hepatic oxidative stress through antioxidative activity in EAC-bearing mice. *Journal of Environmental Pathology Toxicology & Oncology* 26 (4): 245-254.

Chakraborty T, Bhuniya D, Chatterjee M, Rahaman M, Singha D, Chatterjee BN, Datta S, Rana A, Samanta K, Srivastawa S, Maitra S K & Chatterjee M (2007) *Acanthus ilicifolius* plant extract prevents DNA alterations in a transplantable Ehrlich ascites carcinoma- bearing murine model. *World Journal of Gastroenterology* 13 (48): 6538-6548.

Cotran R (1987) The kidney and its collecting system. Chapter 14 in Robbins & Kumar (eds) *Basic Pathology*, W. B. Saunders Company, London, Philadelphia.

Debatin KM, Poncet D & Kroemer G (2002) Chemotherapy: targeting the mitochondrial cell death pathway. *Oncogene* 21: 8786-8803.

Drury R & Wallington E (1980) Carlton's histological techniques. Oxford University Press, New York, 5th edition.

Enzan H, Himeno H, Iwamura S, Saibara T, Onishi S, Yamamoto Y, Miyazaki E & Hara H (1995) Sequential changes in human Ito cells and their relation to postnecrosis liver fibrosis in massive and submassive hepatic necrosis. *Virchows Archiv* 426: 95-101.

Farag AAM & Abdel Dayem SM (2001) Biochemical, histological and ultrastructural studies on the protective effect of vitamin A against carcinogenesic effect of 7, 12-DMBA on the liver of albino rat. *Egyptian Journal of Zoology* 37: 335-368.

Ferreria CG, Epping M, Kruyt FAE & Giaccone G (2002) Apoptosis: target of cancer therapy. *Clinical Cancer Research* 8: 2024-2034.

Fouda FM (2005) Anti-tumor activity of tetrodotoxin extracted from the Masked Puffer fish *Arothron diadematus*. *Egyptian Journal of Biology* 7: 1-13.

Fukuda K, Kojiro M, Chiu Jen FU (1993) Demonstration of extensive chromatin cleavage in transplanted Morris hepatoma 7777 tissue: apoptosis or necrosis? *American Journal of Pathology* 142: 953-946.

George J, Ramesh Rao K, Stern R & Chandrakasan G (2001) Dimethylnitrosamine-induced liver injury in rats: the early deposition of collagen. *Toxicology* 156:129-138.

Grolleau F, Laurence G, Michele B, Bruno L, Marcel P & Erick G (2001) A possible explanation for a neurotoxic effect of the anticancer agent oxaliplatin on neuronal voltage-gated sodium channels. *Journal of Neurophysiology* 85: 2293-2297.

Gupta A, Mazumder UK, Kumar RS & Kumar TS (2004) Anti-tumour activity and anti-oxidant role of *Bauhinia racemosa* against Ehrlich ascites carcinoma in Swiss albino mice. *Acta Pharmacologia Sinica* 25: 1070-1076.

Hagen NA, Fisher K & du Sourich P (2005) Safety of intramuscular tetrodotoxin for inadequately controlled, severe cancer pain. 11th World Congress on Pain (IASP) August 24 2005 Sydney.

Hashimoto S, Koji T, Niu J, Kanematsu T & Nakane PK (1995) Differential staining of DNA strand breaks in dying cells by non-radioactive in situ nick translation. *Archives of Histology & Cytology* 58: 161-170.

Holdaas H, Kopp UC & Dibona GF (1985) Modulation of relex renal vasoconstriction by increased endogenous renal postaglandine synthesis. *Journal of Pharmacology & Experimental Therapeutics* 232: 332-371.

Horn T, Jung J & Christoffersen P (1985) Alcoholic liver injury: early changes of the Disse space in acinar zone 3. *Liver* 6: 301-310.

Kao CY (1966) Tetrodotoxin, saxitoxin and their significance in the study of excitation phenomena. *Pharmacological Reviews* 18: 997-1049.

Kao CY (1972) Pharmacology of tetrodotoxin and saxitoxin. *Federation Proceedings* 13: 1117-1123.

Kawabata T (1978) Food hygiene examination manual Volume 2, Assey method for tetrodotoxins. *Journal of the Food Hygienic Society of Japan* 223-241.

Kiernan JA (1999) Methods for connective tissue: collagen: Masson's trichrome. In Kiernan JS (ed) *Histological and histochemical methods*. 3rd ed. pp 154-155. Bath Press, Somerset.

Lee CK, Park KK, Lim SS, Park JHY & Chung WY (2007) Effects of licorice extract against tumor growth and cisplatin induced toxicity in a mouse xenograft model of colon cancer. *Biological & Pharmaceutical Bulletin* 30 (11): 2191.

Lyu YS, Park SK, Kyungsoon C & Chung JM (2000) Low dose of tetrodotoxin reduces neuropathic pain behaviours in an animal model. *Brain Research* 871: 98-103.

Maity P, Chakrabory S & Bhattacharya P (1999) Antgiogenesis, a putative new approach in glutamine related therapy. *Pathology & Oncology Research* 5 (4): 309-314.

Marcil J, Walezak JS, Guindon J, Ngoe AH, Lu S & Beaulieu P (2006) Antinociceptive effects of tetrodotoxin (TTX) in rodents. *British Journal of Anaesthesia* 96: 761-768.

Maxwell SR (1995) Prospects for the use of antioxidant therapies. *Drugs* 49:345-361.

Navarro J, Obrador E, Carretero J, Petschen I, Avion J, Perez P & Estrela JM (1999) Changes in glutathione status and the antioxidant system in blood and in cancer cells associated with tumor growth *in vivo*. *Free Radical Biology & Medicine* 26: 410-418.

Norbury CJ & Zhivotovsky B (2004) DNA damage – induced apoptosis. *Oncogene* 23: 2797-2808.

Ramakrishna Y, Manohor AI, Mamata P & Shreekant KG (1984) Plants and novel anti-tumor agents: A review. *Indian Drugs* 21: 173-185.

Ramnath V, Kuttan G & Kuttan R (2002) Anti-tumour effect of abrin on transplanted tumours in mice. *Indian Journal of Physiology & Pharmacology* 46: 69-77.

Samanta SM, Alam M, Basu S, Maji T, Roy DK & Jha T (2007) Chemotherapeutic approach to prolonged survival time in combination with immunization and glutamic acid derivatives with anti tumor activity in tumor-bearing mice. *Biological & Pharmaceutical Bulletin* 30 (12): 2334.

Sato C & Izumi N (1989) Mechanism of increased hepatotoxicity of acetaminophen by simultaneous administration of caffeine in the rat. *Journal of Pharmacology & Experimental Therapeutics* 248: 1243-1247.

Sheeja KR, Kuttan G & Kuttan R (1997) Cytotoxic and anti tumor activity of Berberin. *Amala Research Bulletin* 17: 73- 76.

Telbisz A, Kovacs AL & Somosy (2001) Influence of X-ray on the autophagic – lysosomal system in rat pancreatic acini. *Micron* 33 (2): 143-151.

Yamaguchi P (1996) Histopathological and electron microscopic changes in mice treated with puffer fish toxin. *Journal of Toxicological Sciience* 1: 1-14.

الملخص العربي

دراسة هستولوجية وهستوكيميائية عن تأثير الخلايا السرطانية على كبد وكلى الفئران والدور الوقائي المحتمل للتيترودوتوكسين .

سامية محمد عبد الوهاب ، فاطمة مختار فودة
قسم علم الحيوان – كلية العلوم – جامعة الأزهر – فرع البنات و قسم العلوم البيولوجية – كلية البنات – جامعة عين شمس

من المعروف أن العديد من الأدوية المضادة للسرطان لها تأثيرات غير مرغوب فيها مثل سمية الكبد والكلية. أجريت هذه الدراسة للتأكد بالتجربة من تأثير الخلايا السرطانية على كبد وكلية الفئران البيضاء بالإضافة إلى تقييم الدور الوقائي المحتمل للسم المستخلص من جلد سمكة الفهقة والمنتشرة بمياه البحر الأحمر ضد هذا التأثير.
وقد قسمت الفئران إلى ست مجموعات متساوية العدد كالآتي:
المجموعة الضابطة: تم حقنها بمحلول ملحي.
المجموعة الثانية: تم حقنها بجرعة منخفضة غير مميتة من السم ($^1/_{20}$ الجرعة المميتة) .
المجموعة الثالثة: تم حقنها بجرعة عالية غير مميتة من السم ($^1/_{10}$ الجرعة المميتة) .
المجموعة الرابعة: تم حقن الفئران بجرعة قدرها 1 مللي من محلول يحتوي على 2 مليون خلية سرطانية نوعها EAC في التجويف البريتوني .
المجموعة الخامسة : تم حقن الفئران بجرعة قدرها 1 مللي من محلول يحتوي على 2 مليون خلية سرطانية في التجويف البريتوني ثم تم حقنها بجرعة منخفضة غير مميتة من السم ($^1/_{20}$ الجرعة المميتة)
المجموعة السادسة : تم حقن الفئران بجرعة قدرها 1 مللي من محلول يحتوي على 2 مليون خلية سرطانية في التجويف البريتوني ثم تم حقنها بجرعة عالية غير مميتة من السم ($^1/_{10}$ الجرعة المميتة).
تم تشريح الحيوانات لأخذ عينات الكبد والكلية بعد 3 ، 6 ، 9 ، 12 يوم من بداية التجربة لكل المجموعات السابقة . وجهزت قطاعات رقيقة للدراسات الهستولوجية والهستوكيميائية .
وقد أظهرت النتائج أن الحقن بالخلايا السرطانية له تأثير ضار على أنسجة الكبد والكلى حيث أنه يؤدي إلى ظهور فجوات في الخلايا الكبدية مع أنوية منكمشة داكنة الصبغة وظهور مساحات واسعة من النزف الدموي بالكلية وزيادة معنوية في محتوى الجليكوجبن للكبد والكلية ، ولكن عند حقن الفئران بالسم لوحظ أنه يقلل من هذه التأثيرات خصوصاً بعد 3 ، 6 أيام من الحقن بالجرعة المنخفضة الغير مميتة ($^1/_{20}$ الجرعة المميتة). وبالتالي تبرز هذه النتائج إمكانية تضمين هذا السم كنظام علاجي ضد السرطان مع إجراء مزيد من الدراسات عن تأثيراته الجانبية ومدى أمان استخدامه.